International Journal of Applied Electromagnetics and Mechanics 45 (2014) 873–880
DOI 10.3233/JAE-141919
IOS Press

Microprocessing characteristics of inner surface of tube using magnetic functional fluid

Hitoshi Nishida[a,*], Kunio Shimada[b] and Yasushi Ido[c]
[a]*Toyama National College of Technology, Toyama, Japan*
[b]*Fukushima University, Fukushima, Japan*
[c]*Nagoya Institute of Technology, Nagoya, Japan*

Abstract. We proposed a microprocessing method using a magnetic compound fluid for the inner surface of a tube made of a material that is difficult to cut, and clarified the processing characteristics and magnetic field distribution of the tool. The tool inserted into the tube comprises a stack of ring-shaped permanent magnets with spacers between them. There is an almost proportional relationship between the amount of material removed and the processing time, and the processed surface acquires a mirror finish. Moreover, for tools with shorter permanent magnets, the circularity is improved by processing.

Keywords: Magnetic functional fluid, microprocessing, inner tube surface, magnetic field

1. Introduction

Many parts used in aerospace- and energy-related fields are made of stainless steel, super-heat-resistant alloy, or other materials that are difficult to cut, and require high-quality and high-precision processing. Currently, grinding of the inner surfaces of tubes made of such materials is performed using methods such as internal grinding, honing and electrolytic polishing. However, using these methods, it is not easy to achieve shape accuracy at a submicron level, or to produce a processed surface with a small affected layer. For this reason, there is a need for simple methods that enable high-quality, high-precision processing of the inner surfaces of tubes made of difficult-to-cut materials.

In the present study, we propose new microprocessing method using a magnetic compound fluid (MCF) [1,2] for the inner surface of a tube made of a material that is difficult to cut, and clarify the processing characteristics and magnetic field distribution of the tool. To evaluate the processing characteristics, the tube being processed (work piece) was moved back and forth in a reciprocating manner and tools with different magnet lengths were used. The resulting changes in the inner diameter, amount of material removed, circularity, and surface roughness were investigated. The magnetic flux density and its gradient at the inner surface of the work piece were also investigated.

*Corresponding author: Hitoshi Nishida, Toyama National College of Technology, 13 Hongo, Toyama, 939-8630, Japan. Fax: +81 76 493 5439; E-mail: nishida@nc-toyama.ac.jp.

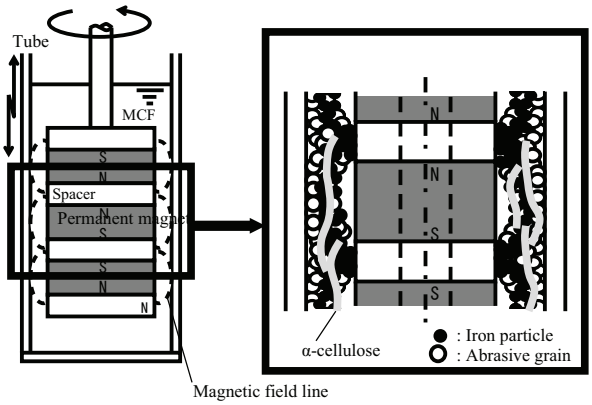

Fig. 1. Schematic diagram of micro processing mechanism.

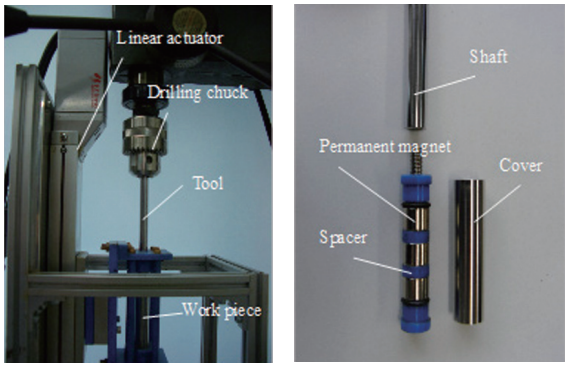

(a) Experimental setup (b) Structure of tool

Fig. 2. Experimental setup and tool.

2. Process principle

Figure 1 shows a schematic diagram of the processing tool and magnetic clusters inside a tube filled with the MCF, including abrasive grains. When a magnetic field is applied to the MCF, an aggregate consisting of iron particles and magnetite particles (magnetic cluster) is formed in the direction of the magnetic force lines. The magnetic clusters are formed in the axial direction of the outer surface of the tube of the permanent magnet. Magnetic buoyancy causes the abrasive grains to move to locations where there is little magnetic field strength, i.e., the inner side of the tube [3]. It is thought that processing occurs because the magnetic clusters that form in the axial direction of the outer surface of the tube of the permanent magnet apply a force in the radial direction of the abrasive grains that have collected on the inner surface of the tube, and because of the relative movement between these grains and the inner surface of the tube.

3. Grinding experimental setup

3.1. Experimental setup and conditions

Figure 2 shows the experimental setup and the structure of the tool. The setup comprised the work piece, which contained an MCF in which abrasive grains had been mixed, a power slider that holds the work piece, a tool composed of permanent magnets and spacers (made of MC nylon), as well as a drill press that caused the tool to rotate. The slider enabled reciprocating movement of the work piece. As shown in Fig. 2(b), the tool comprised ring-shaped permanent magnets placed in a stacked configuration with like poles facing each other, and with spacers between them. The permanent magnets used in the tool were neodymium magnets ($Nd_2Fe_{14}B$) with an outer diameter of 12 mm and an inner diameter of 6 mm. For the experiments, the permanent magnets were covered with a nonmagnetic stainless steel tube with a thickness of 0.7 mm. The outer diameter of the tool was 13.4 mm. Table 1 shows the three types of tools (Type A, B and C) used in the present study, as well as the experiment conditions.

3.2. Testing fluid, work pieces and measurement method

For the magnetic fluid that served as the mother solution of the MCF, we used a kerosene-based magnetic fluid (MSGS60, Ferrotec). The MCF was prepared by adding carbonyl iron powder (HQ,

Table 1
Tool type and experimental conditions

Type	A	B	C
Size of permanent magnet (mm)	$\Phi 12 \times \Phi 6 \times 10$	$\Phi 12 \times \Phi 6 \times 5$	$\Phi 12 \times \Phi 6 \times 3$
Magnetic flux density of surface (mT)	420	370	300
Number of magnet	3	3	5
Thickness of spacer (mm)	5	2.5	1.5
Tool length (mm)	40	20	21
Frequency of reciprocating motion (Hz)	0.33	0.67	0.67
Amplitude of reciprocating motion (mm)	7.5	3.75	2.25
Structure of tool	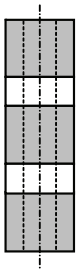	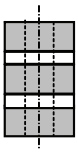	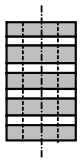

Table 2
Components of testing fluid

MF (MSGS60)	39.2 wt.%
Iron powder (1.2 μm, HQ)	30.4 wt.%
Al_2O_3 abrasive (3 μm)	20.0 wt.%
α-cellulose	6.4 wt.%
Kerosene	4.0 wt.%

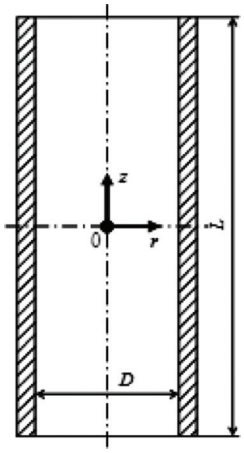

Fig. 3. Coordinate system.

mean particle diameter: 1.2 μm, BASF) to this fluid. The test fluid was prepared by mixing this MCF with non-agglutinating pure alumina powder (AP-D, mean particle diameter: 3 μm, Marumoto Struers K.K.) as non-magnetic abrasive grains, and α-cellulose (α-Cellulose (fibriform), Nakalai Tesque, Inc.), which acts to increase the shear strength of the magnetic clusters. In the experiments, 5.3 ml of the test fluid was used for each experimental condition. Table 2 shows the test fluid components used in this study. The work pieces used were stainless steel tubes (SUS304BA), and one tube was used for each experimental condition. The tubes had an inner diameter of 14.9 mm, an outer diameter of 17.3 mm, and a length of 100 mm. The mean value of the arithmetic mean roughness Ra_0, a parameter used to evaluate the surface roughness prior to processing of the inner surface of the tube, was 0.287 μm, and the mean value of the circularity (A two-dimensional geometric tolerance that controls how much a feature can deviate from a perfect circle) C_0 was 13.5 μm.

Figure 3 shows the coordinate system for the work piece. The inner diameter and circularity were measured using a three-dimensional measuring apparatus (XYZAX SVA fusion, Tokyo Seimitsu Co.,

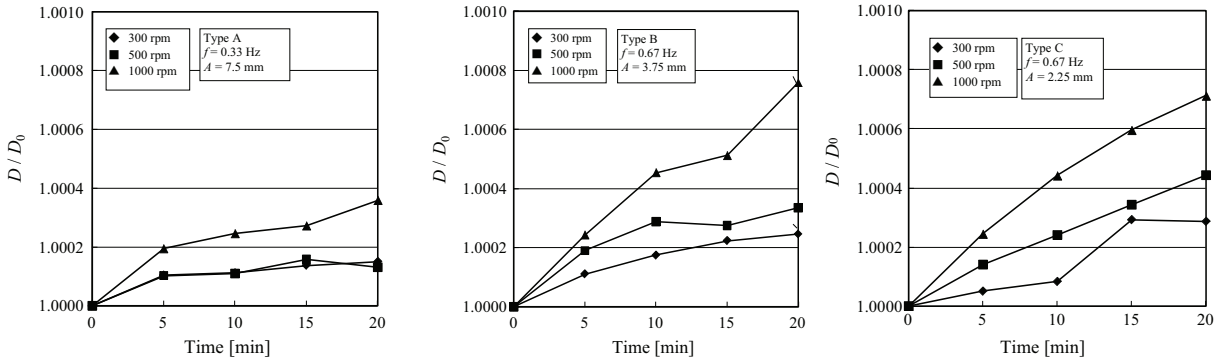

(a) Type A (b) Type A (c) Type A

Fig. 4. Time change of internal diameter ratio.

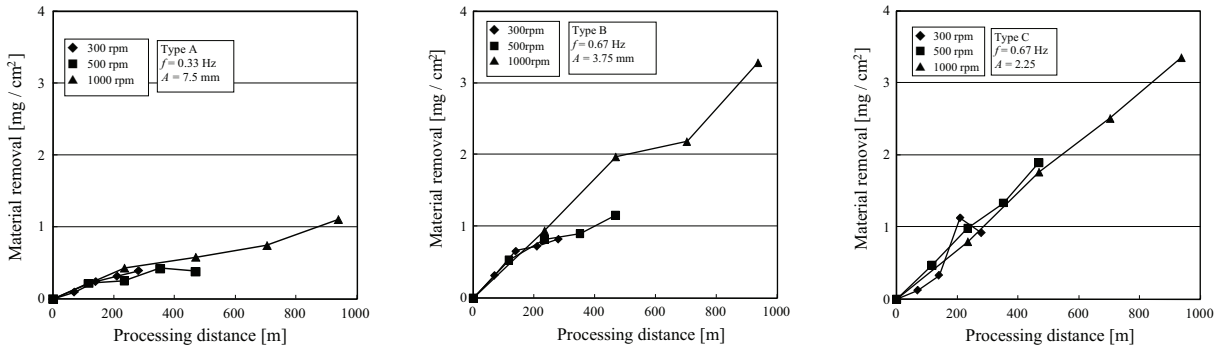

(a) Type A (b) Type B (c) Type C

Fig. 5. Relation between material removal and processing distance.

Ltd.). We also measured surface roughness inside the tube, using an instrument for surface roughness measurement (Surfcom 1900DX3, Tokyo Seimitsu Co., Ltd.). The amount of material removed was determined from the difference in the mass of the work piece before and after processing. For the mass measurements, electronic scales (GR-202, A & D Co., Ltd., minimum display 0.01 mg) were used.

To measure the magnetic flux density distribution of the tool, a Gauss meter (Model 425 Gauss meter, Lake Shore) was used. The magnetic flux density in the radial direction was measured using a transverse probe (HMNT-4E04-VR, Lake Shore). Measurement in the axial direction was carried out using an axial probe (HMMA-0604-TH, Lake Shore). To determine the distribution of the magnetic flux density of the tool, at $r = 7.35$ mm and 7.45 mm (positions corresponding to the inner surface of the tube) and 7.55 mm, the magnetic flux density Br in the radial direction and Bz in the axial direction were measured at intervals of 0.25 mm along the axial direction of the tube.

4. Processing test results

4.1. Changes in the inner diameter and amount of material removed

Figure 4 shows the ratio of the inner diameter after and before processing, D/D_0, as a function of the processing time, for the Type A, Type B, and Type C tools at various rotation speeds. Here, D_0 is the

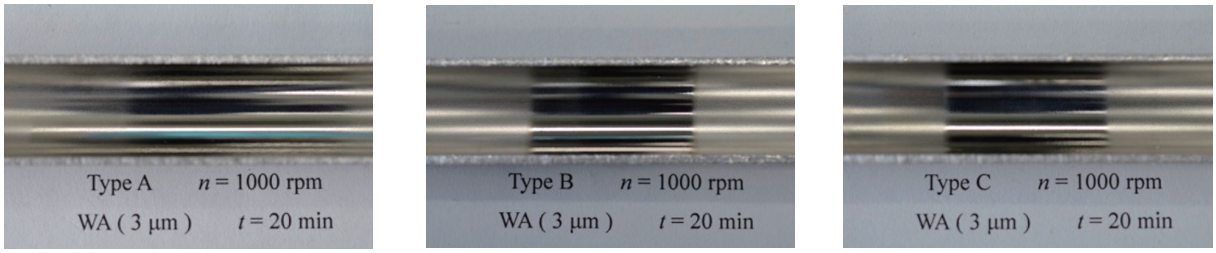

(a) Type A (b) Type B (c) Type C

Fig. 6. Photos of processed surfaces.

inner diameter before processing, and D is the inner diameter after processing. In order to be able to directly compare changes in the inner diameter for each experiment condition, the inner diameter ratio D/D_0 was therefore used. As the rotation speed increased, the change in the inner diameter ratio also increased. However, with the Type A tool, which had longer permanent magnets, the inner diameter ratio was almost the same for $n = 300$ and 500 rpm. With the Type B tool and $n = 1000$ rpm, the inner diameter increased by 11.3 μm after 20 min of processing.

Figure 5 shows the relation between the amount of material removed per unit area as a function of the processing distance for each of the tools. For all of the tools, a proportional relationship was observed. With operations such as polishing, it is known that the amount of material removed is proportional to the processing distance, and as the proportional constant increases, the material removal increases correspondingly. The gradient shown in Fig. 5 expresses this proportional constant, and for the tool shown here, the larger the gradient, the larger the amount of material removed. For the Type A tool, the gradient was small, whereas it was larger for the Type B and Type C tools. It was also found that the amount of material removed was almost the same for the Type B and Type C tools.

4.2. Changes in surface roughness and circularity

Figure 6 shows photographs of the inner surfaces of the tubes after 20 min of processing at a tool rotation speed of $n = 1000$ rpm, for each of the tools. The roughness curves at this point are shown in Fig. 7. For the Type B and Type C tools, it can be seen that the inner surface of the tube has a mirror finish within the processed region (the region within which the tool moved reciprocally). Thus, in addition to increasing the inner diameter, this processing method caused the surface to become smooth.

Figure 8 shows the ratio of the circularity after and before processing, C/C_0, as a function of the processing time, for each of the tools. Here, C_0 is the circularity before processing, and C is the circularity after processing. With the Type A tool, which had longer permanent magnets, no change is seen in the circularity ratio. With the Type B tool, the circularity improved up to a processing time of 10 min, but no further improvement occurred after that point. With the Type C tools, however, it can be seen that the circularity continued to improve. After 20 min of processing, the circularity had improved from 9.5 to 5.6 μm. The improvement in circularity is thought to be an important feature of this processing method. Tools with shorter permanent magnets have a magnetic field distribution that is more susceptible to the self-centering effect of the tool, leading to an improvement in circularity.

5. Magnetic field distribution

Figure 9 shows the distribution of the magnetic flux density B (absolute value) at a position ($r = 7.45$ mm) corresponding to the inner surface of the permanent magnet in the center of the tool. The

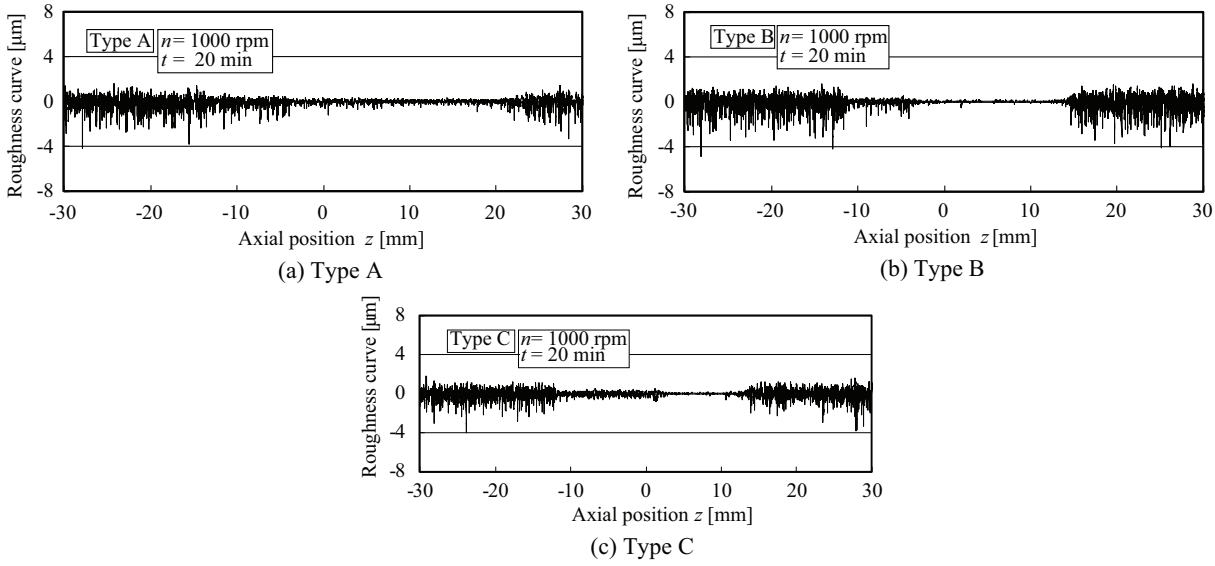

Fig. 7. Roughness curves of processed surfaces.

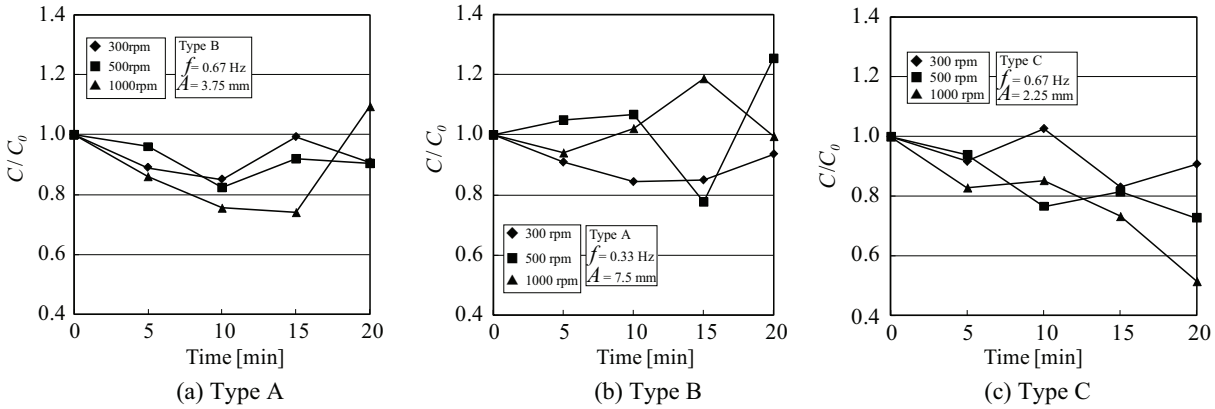

Fig. 8. Time change of the circularity ratio.

x-axis indicates the distance along the axial direction from the center of the permanent magnet for each of the tools. For all of the tools, the magnetic flux density is lower at the center of the side surface of the permanent magnet. With the Type A and Type B tools, there is a peak at the end surface of the permanent magnet, and the density then decreases at the center of the spacer field. With the Type C tool, however, there is a peak in the spacer field. For the Type C tool, it is thought that abrasive grains gather easily at center of the side surface of the permanent magnet.

If a magnetic body is in a nonuniform magnetic field, the force acting on the body is expressed by the product of the magnetic moments and the gradients of the magnetic fields. Based on this concept, Fig. 10 shows the relationship between the magnetic flux density and its gradient at the center of the longitudinal direction of the magnet as well as the end of the magnet and the center of the longitudinal direction of the spacer, regarding the processed inner surface for the permanent magnets of each tool. It can be seen that the changes in the radial direction of the magnetic flux density component at each position are large.

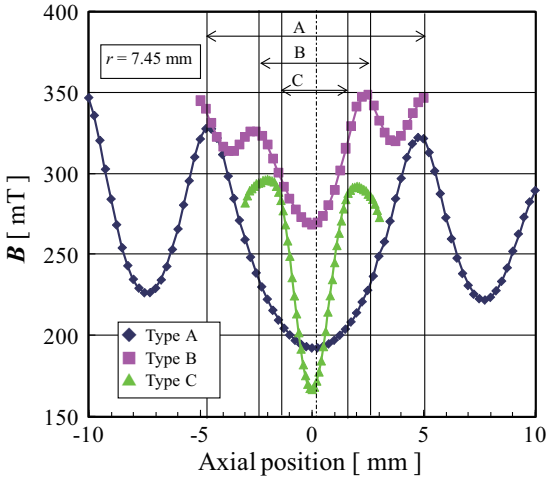

Fig. 9. Distribution of magnetic flux density.

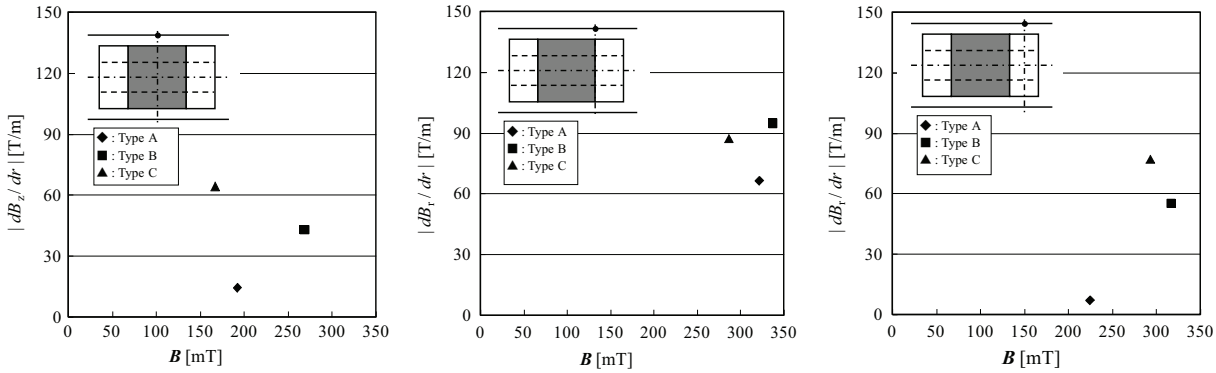

(a) At the center of the permanent magnet (b) At the edge of the permanent magnet (c) At the center of the spacer

Fig. 10. Relation of magnetic flux density to gradient.

Figure 10(a) shows the magnetic field characteristics at the center in the longitudinal direction of the permanent magnet; it can be seen that the magnetic flux density gradient in the Type A tool is small. Figure 10(b) shows the magnetic field characteristics at the end surface of the permanent magnet. The magnetic flux densities and gradients for the three types of tools are large, so that the material removal rate is high at the tool end. The magnetic flux density and its gradient are largest for the Type B tool, which is consistent with this tool producing the largest change in the internal diameter. Figure 10(c) shows the magnetic field characteristics at the center in the longitudinal direction of the spacer, and it can be seen that the magnetic flux density gradient for the Type A tool is close to zero. However, for the Type C tool, the magnetic flux density gradient is comparatively large. This may be the cause of the improvement in circularity in Type C.

6. Conclusion

We proposed new microprocessing method for the inner surface of a tube using an MCF and clarified

the processing characteristics. The results can be summarized as follows:

(1) The inner diameter of the tube increases with processing time. There is an almost proportional relationship between the amount of material removed and the processing time, and the processed surface acquires a mirror finish.
(2) With the Type C tool, which has shorter permanent magnets, the circularity is improved automatically by processing. After 20 min of processing, the circularity improves from 9.5 to 5.6 μm.
(3) Both the magnetic flux density and its gradient are larger at the end surface of the permanent magnet, and the highest values are obtained for the Type B tool. This denotes the significant change of the inner diameter produced by our used tool.

References

[1] K. Shimada, T. Fujita, H. Oka, Y. Akagami and S. Kamiyama, Hydrodynamic and magnetized characteristics of MCF, *Trans Jpn Soc Mech Eng* **67–664** B(2001), 3034–3040.
[2] K. Shimada, Y. Matuo, K. Yamamoto and Y. Wu, A nw float-polishing technique with large clearance utilizing magnetic compound fluid, *IJ Abrasive Technology* **1 Nos.3/4** (2008), 302–315.
[3] Y. Ido, T. Yamaguchi and H. Nishida, Numerical analysis of the polishing process of inner tube wll using micron-size particles in magnetic fluids, *Materials Science Forum* **670** (2011), 110–117.